Oncogene
https://doi.org/10.1038/s41388-019-0973-5

ARTICLE

ALK^{ATI} interacts with c-Myc and promotes cancer stem cell-like properties in sarcoma

Bu-Shu Xu[1] · Huo-Ying Chen[1,2] · Yi Que[1] · Wei Xiao[1] · Mu-Sheng Zeng[3] · Xing Zhang[1]

Received: 30 August 2018 / Revised: 11 January 2019 / Accepted: 16 May 2019

Abstract

Soft tissue sarcoma (STS) is a highly malignant tumor with limited targeted therapies. A novel anaplastic lymphoma kinase (ALK) transcript, *ALK*^{ATI}, was identified recently and could be targeted by ALK inhibitors in melanoma. However, the clinical and functional role of aberrant *ALK*^{ATI} expression in STS remains unknown. Here we demonstrate that as a new *ALK* transcript, *ALK*^{ATI} is frequently found in STS. *ALK*^{ATI} expression correlates with a lower probability of progression-free survival in STS patients. Compared with the other *ALK* isoforms, ALK^{ATI} expresses not only in the cytoplasm, but also in the nucleus of sarcoma cells. Functionally, overexpression of *ALK*^{ATI} promoted cancer stem cell (CSC)-like properties in sarcoma cells by promoting sphere formation and upregulating the expression of stem cell markers. Moreover, the ALK inhibitors not only suppressed the oncogenic functions of *ALK*^{ATI} but also attenuated *ALK*^{ATI}-induced CSC-like properties by reducing the expression of stem cell markers such as c-Myc, ABCG2, BMI1, and OCT4 both in vitro and in vivo. Furthermore, ALK^{ATI} interacted with c-Myc and increased the binding of c-Myc to the *ABCG2* promoter, resulting in the induction of stem cell-like properties. Together, these findings indicate that *ALK*^{ATI} may be a potential prognostic marker and therapeutic target for STS patients harboring such *ALK* aberrations.

Introduction

Soft tissue sarcoma (STS) is a solid malignant tumor accounts for ~1% of adult cancers [1]. STS treatment failures mainly result from local recurrence and distant metastasis [2, 3], but the option of therapeutic agents for advanced STS limits. Although new drugs such as pazopanib [4], trabectedin [5], eribulin [6], and olaratumab [7] have been approved for the treatment of advanced STS in recent years, the clinical effects are less than satisfaction, which restrict their applications [8]. Therefore, further efforts on discovering new therapeutic targets for STS personalized treatments become urgently necessary.

Aberrations in the oncogene anaplastic lymphoma kinase (ALK) have emerged as potentially relevant biomarkers and therapeutic targets in several solid and hematologic tumors [9]. The most common *ALK* aberrations includes the *TPM3-ALK* [10], *EML4-ALK* [11], and *NPM-ALK* [12] translocations and the *F1147L* [13] mutation. Although some clues revealed that a few *ALK* aberrations might be present in several STS subtypes and result in poor prognosis [14–20], they have not been confirmed in most of the STS subtypes yet and the clinical and functional role of *ALK* in STS remains uncertain. Therefore, further investigation is required to uncover more possible *ALK* aberrations in STS.

Recently, a novel transcript of *ALK* was identified in melanoma. This transcript consists primarily of the intracellular tyrosine kinase domain and, as it initiates from a de novo alternative transcriptional initiation (ATI) site in *ALK* intron 19, was accordingly named *ALK*^{ATI} [21].

These authors contributed equally: Bu-Shu Xu, Huo-Ying Chen

Supplementary information The online version of this article (https://doi.org/10.1038/s41388-019-0973-5) contains supplementary material, which is available to authorized users.

✉ Xing Zhang
zhangxing@sysucc.org.cn

[1] Melanoma and Sarcoma Medical Oncology Unit, State Key Laboratory of Oncology in South China, Collaborative Innovation Center for Cancer Medicine, Sun Yat-sen University Cancer Center, 651 Dongfeng Road East, Guangzhou 510060, China

[2] Department of Laboratory Medicine, The Second Affiliated Hospital of Guilin Medical University, Guilin 541100, China

[3] State Key Laboratory of Oncology in South China, Collaborative Innovation Center for Cancer Medicine, Sun Yat-sen University Cancer Center, 651 Dongfeng Road East, Guangzhou 510060, China

Published online: 28 August 2019

ALK^{ATI} is expressed in ~11% of melanomas and sporadically in other cancer types, but is not expressed in normal tissues [21, 22]. Whether *ALK*^{ATI} expressed in STS has not been reported before and *ALK*^{ATI} currently could not be detected by routine tests designed for the known *ALK* fusion genes or mutations. As *ALK*^{ATI}-driven tumors are sensitive to ALK inhibitors [21], detection of *ALK*^{ATI} in STS represents a therapeutic opportunity for patients harboring such tumors. In addition, the identification of this type of *ALK* aberration is an important step in understanding the pathology of STS.

Therefore, the purpose of the current study was to examine the presence of *ALK*^{ATI} in STS and to clarify its functional role. We found that *ALK*^{ATI} was present in STS and that *ALK*^{ATI} expression correlated with a poor prognosis. Furthermore, we demonstrated that *ALK*^{ATI} not only contributed to tumorigenesis but also promoted cancer stem cell (CSC)-like properties by interacting with c-Myc and increasing the binding of c-Myc to the *ABCG2* promoter in STS. Our findings suggest that ALK kinase inhibitors may become a treatment option for patients with *ALK*^{ATI}-driven sarcomas.

Results

ALK^{ATI} is present in STS and correlates with a poor prognosis

To evaluate the clinical influence of *ALK*^{ATI} in STS, we examined the presence of *ALK*^{ATI} in fresh STS biopsy specimens by real-time PCR assays with sequence-specific probes and two primers constructed for *ALK* intron 19 and exons 20–29. We found that *ALK*^{ATI} occurred in 31.6% (12/38) of many different histologic subtypes of STS. Furthermore, we analyzed the clinical significance of *ALK*^{ATI} in 38 STS patients with available clinical follow-up data and found a correlation between the presence of *ALK*^{ATI} and clinicopathologic features, including tumor grade ($P = 0.010$) and tumor size ($P = 0.036$) (Table 1). Furthermore, patients with *ALK*^{ATI} mRNA expression demonstrated a significantly lower probability of progression-free survival (PFS) ($P < 0.05$, Fig. 1a). These results indicate that the *ALK*^{ATI} isoform exists in STS patients and that *ALK*^{ATI} may be a novel prognostic biomarker for STS patients.

We also examined endogenous mRNA and protein expression of *ALK*^{ATI} in various sarcoma cell lines, including HT1080, U2197, and SK-LMS-1 cell lines. However, we found that in these sarcoma cell lines, the expression level of either mRNA (data not shown) or protein (Fig. 1b) of *ALK*^{ATI} and wild-type *ALK* is undetectable.

Table 1 Correlation of *ALK*^{ATI} expression and patient features of STS

Characteristic	*ALK*^{ATI}-positive ($N = 12$)	*ALK*^{ATI}-negative ($N = 26$)	*P*
Age			0.553
<60	3 (25.0%)	9 (34.6%)	
≥60	9 (75.0%)	17 (65.4%)	
Sex			0.126
Female	3 (25.0%)	11 (42.3%)	
Male	9 (75.0%)	15 (57.7%)	
Tumor grade			0.010
G1 + G2	4 (33.3%)	20 (76.9%)	
G3	8 (66.7%)	6 (23.1%)	
Tumor size			0.036
≤5 cm	3 (25.0%)	16 (61.2%)	
>5 cm	9 (75.0%)	10 (38.8%)	
Tumor site			0.510
Trunk & extremity	8 (66.7%)	12 (46.2%)	
Head/neck & intra-abdominal	4 (33.3%)	14 (53.8%)	
Tumor depth			
Superficial	5 (41.7%)	8 (44.4%)	
Deep	7 (58.3%)	18 (56.6%)	
AJCC stage			0.106
I+II	5 (41.7%)	18 (69.2%)	
III+IV	7 (58.3%)	8 (30.8%)	

N number, *AJCC* American Joint Committee on Cancer

ALK^{ATI} localizes to both the cytoplasm and the nucleus in STS

We examined an additional cohort of 142 paraffin-embedded sarcoma specimens for ALK expression by immunohistochemistry (IHC) and we found 20 cases that were ALK labeled in this cohort (Supplementary Table 1). In 11 cases, the ALK staining pattern was predominantly cytoplasmic, but nuclear staining was also observed (Fig. 1c). As previously reported [21], ALK^{ATI} expressed in both the nucleus and the cytoplasm, whereas wild-type ALK and the other ALK isoforms mainly expressed in the cytoplasm and/or at the cell membrane. Nuclear localization was a typical biomarker of ALK^{ATI}. The identification of ALK nuclear staining observed here further confirmed that ALK^{ATI} expressed in STS. To further address the expression pattern of ALK^{ATI}, we stably transduced HT1080 cell lines with *ALK*^{ATI}, negative control (NC) (empty vector), wild-type *ALK*, or *NPM-ALK*. Using immunofluorescence, we found that ALK^{ATI} expressed in both the nucleus and the cytoplasm, whereas wild-type ALK and NPM-ALK were mainly present in the cytoplasm and/or at the cell membrane (Fig. 1d). These observations suggest that the nuclear and

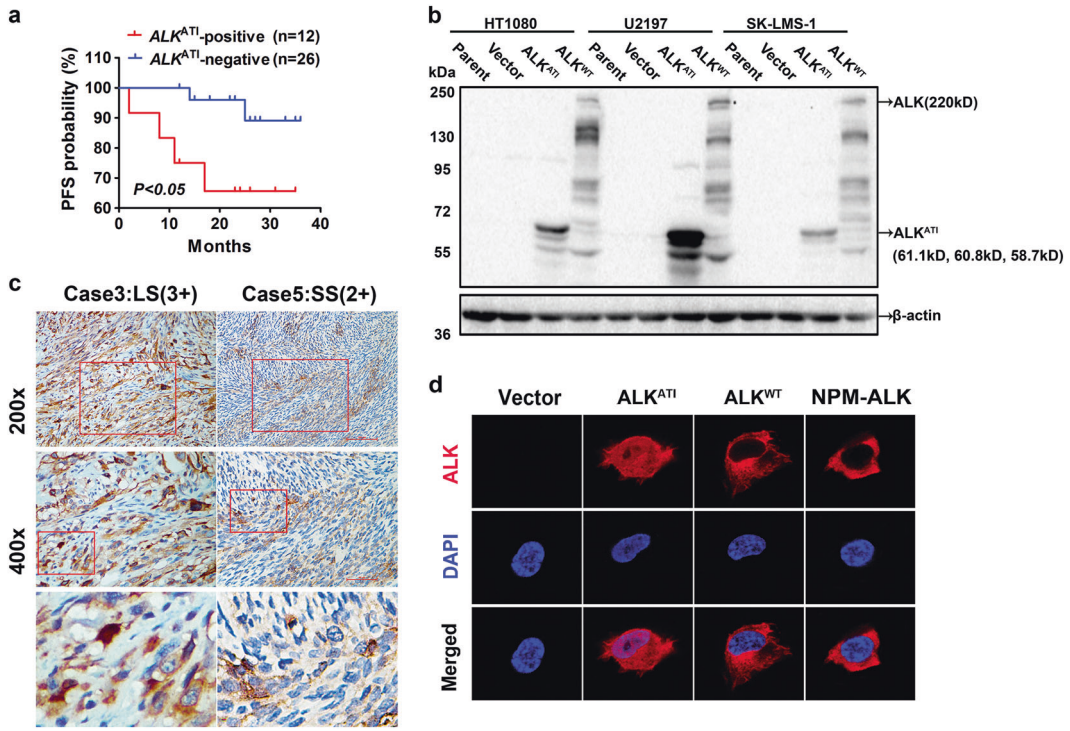

Fig. 1 Expression and prognostic significance of *ALK*^{ATI} in soft tissue sarcomas. **a** Prognostic significance of *ALK*^{ATI} mRNA expression. The expression of *ALK*^{ATI} in soft tissue sarcoma (STS) biopsy specimens was detected using real-time PCR. Kaplan–Meier and log-rank analyses for progression-free survival (PFS) of STS patients ($n = 38$) with available clinical follow-up data identified two subgroups of patients with significantly different probabilities of PFS ($P < 0.05$). **b** Western blotting analysis of the protein expression of exogenous *ALK*^{ATI} and *ALK*^{WT} in human sarcoma cell lines. Results shown are representative of three independent experiments. **c** Immunohistochemical staining for ALK in STS tissues. Both nuclear and cytoplasmic ALK labeling is observed in Leiomyosarcoma (LS, case 3), and synovial sarcoma (SS, case 5) tissues at high magnification, which is indicated by rectangles at ×400 and ×200 magnification. **d** Immunofluorescent staining of ALK in HT1080 cells expressing the indicated *ALK* isoforms or vector. Original magnification: ×600

cytoplasmic ALK^{ATI} expression may have a different function from the other ALK isoforms.

ALK^{ATI}-expressing sarcoma cells exhibited stronger CSC-like properties

ALK kinase plays an important role in the growth and proliferation of tumor cells [9]. To establish the differences in *ALK*^{ATI} function as compared with the other *ALK* isoforms, we first examined the growth and proliferation of stably transduced sarcoma cells by MTT and colony formation assays, including HT1080, U2197, and SK-LMS-1. Our results showed that these *ALK*^{ATI}-expressing sarcoma cells grew faster and produced more colonies than the empty vector-infected cells. However, the growth and proliferation of *ALK*^{ATI}-infected cells was similar to that of the wild-type *ALK*- and *NPM-ALK*-infected cells (Supplementary Fig. 1a, b). The observed oncogenic properties of *ALK*^{ATI} are consistent with a previous report [21]. These results indicate that in comparison to the wild-type *ALK* and *NPM-ALK*, the functional differences of *ALK*^{ATI} are not related to cells growth and proliferation.

Multiple genetic alterations that control cell proliferation and differentiation lead to abnormal proliferation and malignant transformation of cancer cells with stem cell-like properties [23, 24]. To determine whether *ALK*^{ATI} has any effect on CSC-like properties, we performed a sphere formation assay using empty vector-, wild-type *ALK*-, *NPM-ALK*-, or *ALK*^{ATI}-overexpressing sarcoma cells. As shown in Fig. 2a, b, HT1080 and U2197 cells expressing *ALK*^{ATI} formed more and larger spheres than cells expressing the empty vector, wild-type *ALK*, or *NPM-ALK*. We examined the mRNA expression levels of stem cell markers, including *c-Myc*, *ABCG2*, *BMI1*, *OCT4*, *CD44*, and *CD133*, by real-time PCR. Our results showed that overexpression of *ALK*^{ATI} upregulated mRNA expression levels of these stem cell markers in primary spheres (Fig. 2c, d).

As reported, CSCs play an important role in resistance to cancer therapy [25]. We further investigated that *ALK*^{ATI}-expressing sarcoma cells formed more colonies after treatment with 0.5 μM Cisplatin (DDP) or irradiation with 3 or 6 Gy than controls (Supplementary Fig. 1c, 1d), suggesting that the *ALK*^{ATI} isoform confers distinct radioresistant phenotype.

Taken together, these results suggest that *ALK*^{ATI} enhances CSC-like properties, which might result in the resistance of sarcoma cells to both radiotherapy and chemotherapy.

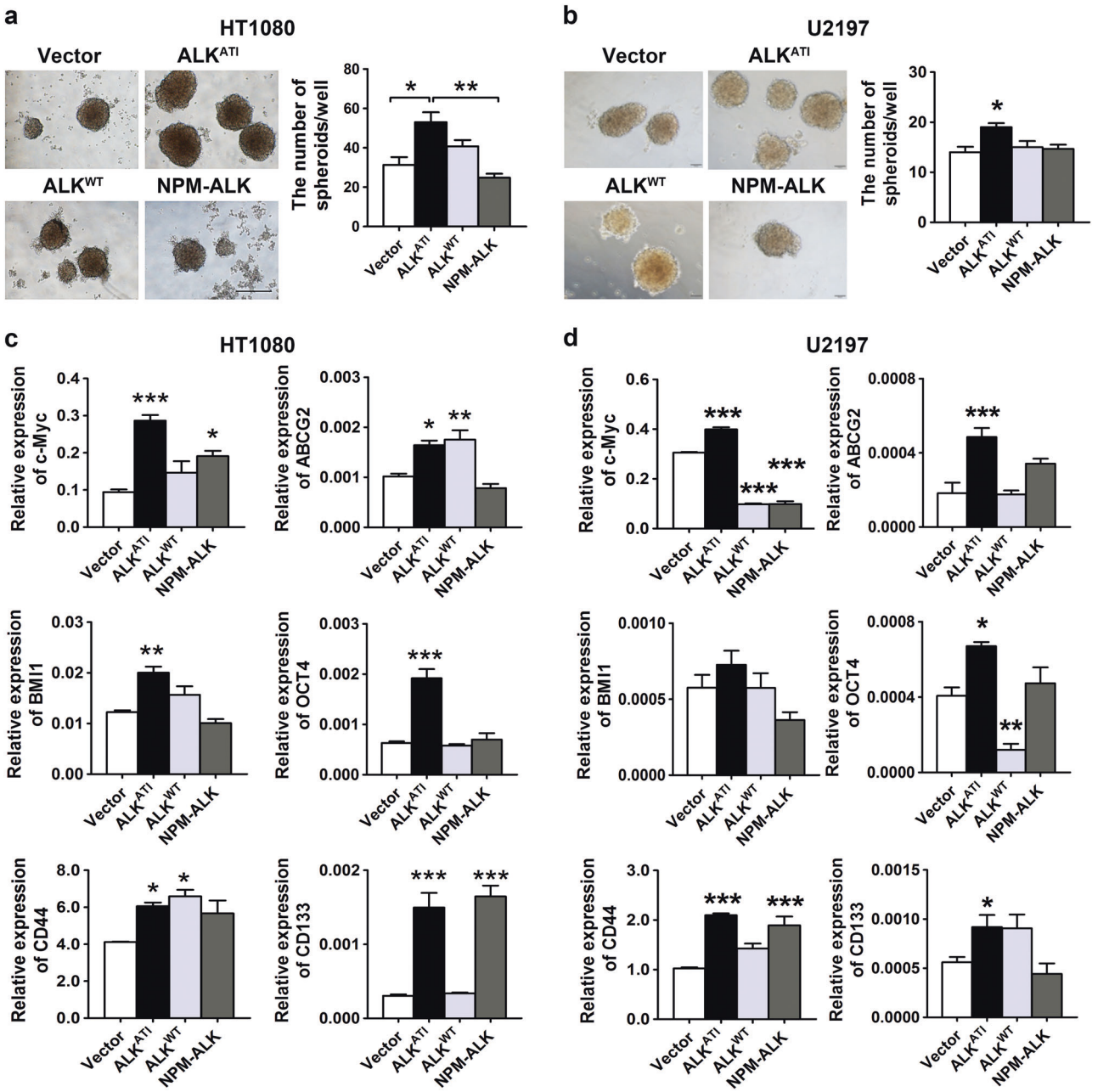

Fig. 2 CSC-like properties induced by *ALK*^{ATI} in both HT1080 and U2197 cells. **a**, **b** Primary sphere formation of HT1080 and U2197 cells expressing the indicated *ALK* isoforms or vector. Magnification: ×100. The numbers of spheres formed by these cells are shown in the right panel; $n = 3$ wells per group. **c**, **d** Real-time PCR detection of stem cell markers in primary sphere cells. Gene expression was normalized to the geometric mean of the housekeeping gene *β-actin*. Data are shown as mean ± SD. $^{*}P < 0.05$, $^{**}P < 0.01$, $^{***}P < 0.001$ vs. Vector group using one-way ANOVA analysis followed by Bonferroni post hoc test. Results shown are representative of three independent experiments

ALK^{ATI}-expressing primary sphere sarcoma cells showed a greater capacity for subcultured sphere formation

We further evaluated the capacity for subcultured sphere formation of sarcoma primary sphere cells expressing *ALK*^{ATI} or empty vector. As shown in Fig. 3a, b, cells dissociated from the *ALK*^{ATI}-expressing HT1080 and U2197 sphere primary, secondary, or third generation cells were shown to be capable of repeatedly forming spheres, while the empty vector groups were gradually lost the capacity. Meanwhile, the subcultured *ALK*^{ATI}-expressing HT1080 and U2197 sphere cells retained high *c-Myc*, *ABCG2*, *BMI1*, *OCT4*, *CD44*, and *CD133* expression (Fig. 3c, d). These results indicate that subcultured sphere cells expressing *ALK*^{ATI} maintain strong CSC-like characteristics.

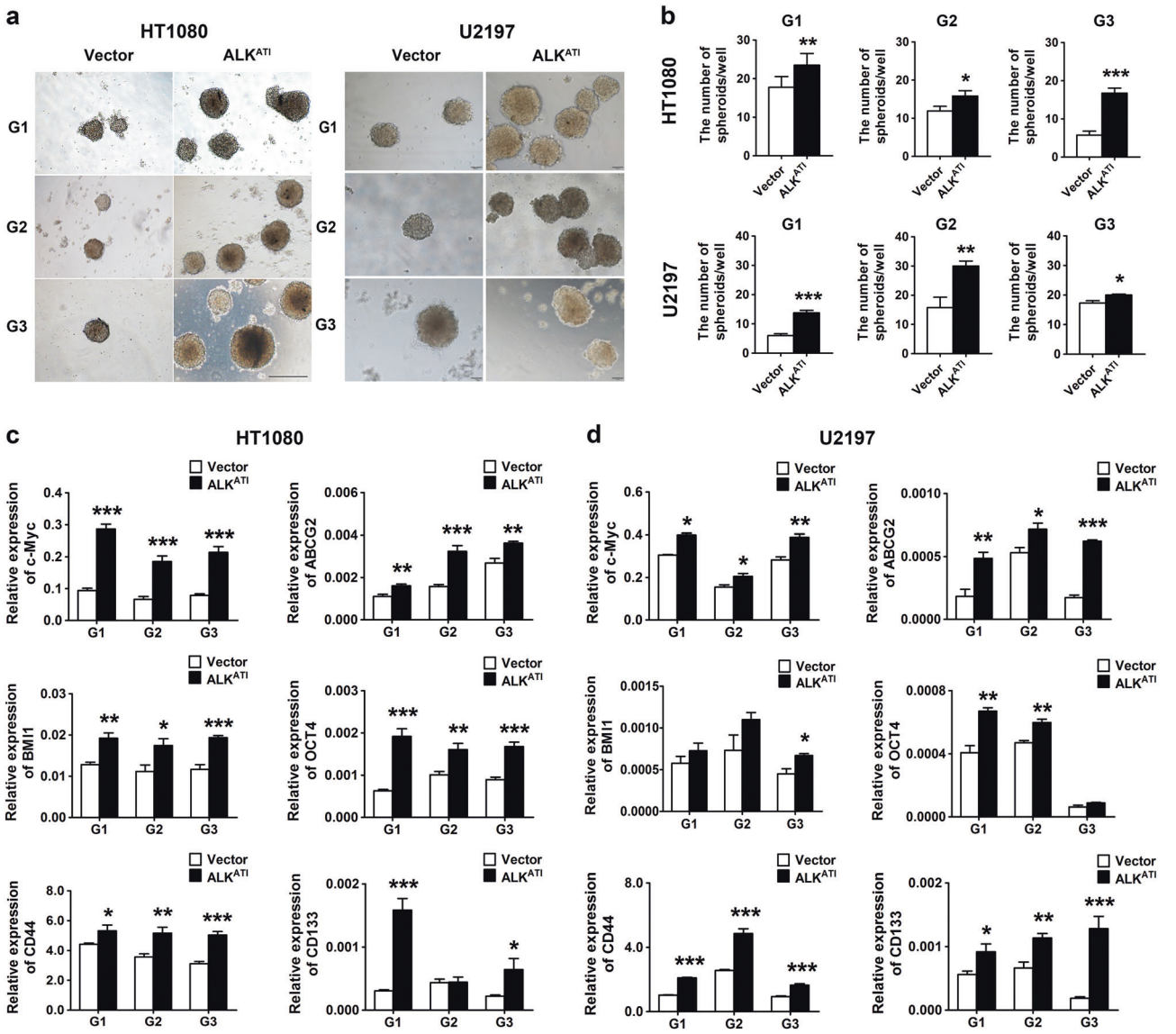

Fig. 3 CSC-like properties maintained by *ALK*^{ATI} in both HT1080 and U2197 subcultured sphere cells. **a** Subculture sphere formation of HT1080 and U2197 cells expressing *ALK*^{ATI} or vector. Magnification: ×100. Cells were dissociated from the primary or secondary spheres using 0.02% EDTA and subcultured for new sphere formation. G1 indicates the primary generation, G2 indicates the second generation, and G3 indicates the third generation. $n = 4$ wells per group. **b** The numbers of subcultured spheres are shown; $n = 3$ wells per group. **c, d** Real-time PCR detection of stem cell marker expression in related subcultured sphere cells. Gene expression was normalized to the geometric mean of the housekeeping gene *β-actin*. Data are shown as mean ± SD. $^{*}P < 0.05$, $^{**}P < 0.01$, $^{***}P < 0.001$ vs. Vector group using two-tailed Student's *t*-test. Results shown are representative of two independent experiments

ALK inhibitors suppressed the expression of stem cell markers enhancing by *ALK*^{ATI}

ALK^{ATI} has been reported to be sensitive to ALK inhibitors [21]. Here, we used crizotinib as well as ceritinib to treat *ALK*^{ATI}-expressing HT1080 cells and found that they inhibited growth and colony formation in *ALK*^{ATI}-expressing HT1080 cells (Fig. 4a, b). These ALK inhibitors also declined the phosphorylation of ALK^{ATI} and the downstream effectors AKT and mTOR in a concentration-dependent manner (Fig. 4c), whereas they did not affect this signal pathway in vector-transfected HT1080 cells (Supplementary Fig. 2d). To determine whether ALK inhibitors impair the CSC-like properties of *ALK*^{ATI}-expressing HT1080 cells, we examined the protein expression levels of stem cell markers, including c-Myc, ABCG2, BMI1, and OCT4, in HT1080 cells overexpressing *ALK*^{ATI} following crizotinib or ceritinib treatment. Expression of these stem cell markers was reduced in *ALK*^{ATI}-expressing HT1080 cells treated with crizotinib or ceritinib (Fig. 4d), even after

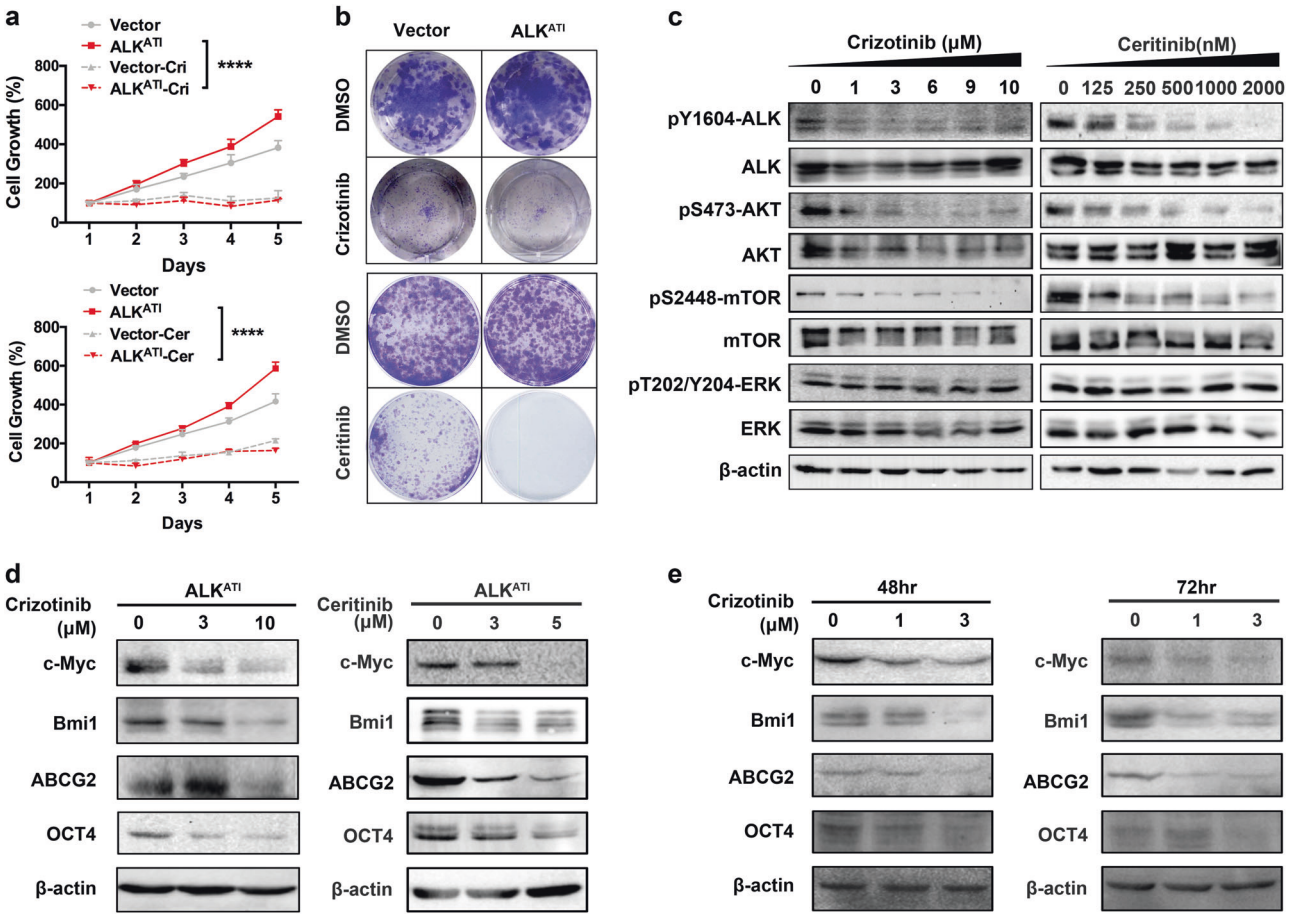

Fig. 4 Inhibitory effect of ALK inhibitors on HT1080 cells expressing ALK^{ATI}. **a** The growth curves of HT1080 cells stably expressing ALK^{ATI} or vector based on the MTT assay; cells were cultured for 5 days post treatment with 1 μM of crizotinib or ceritinib or vehicle (DMSO); $n = 5$ wells per group. An asterisk refers to differences between DMSO and crizotinib or ceritinib treatment. Data are shown as mean ± SD. $^{****}P < 0.0001$ by one-way ANOVA analysis followed by Bonferroni post hoc test. **b** Representative images of colonies formed by HT1080 cells stably expressing ALK^{ATI} or vector. Cells were cultured for 7–10 days post treatment with an IC_{25} concentration of crizotinib or ceritinib; $n = 3$ wells per group. **c** Representative western blotting images of ALK^{ATI} phosphorylation and downstream AKT, mTOR, and ERK expression in ALK^{ATI}-expressing HT1080 cells treated with the indicated concentration of crizotinib or ceritinib for 3 h. **d** Representative western blotting for stem cell markers in HT1080 cells stably expressing ALK^{ATI}. Cells expressing ALK^{ATI} were treated with the indicated concentration of crizotinib or ceritinib for 24 h. **e** Representative western blotting for stem cell markers in HT1080 cells stably expressing ALK^{ATI}. Cells expressing ALK^{ATI} were treated with the indicated concentration of crizotinib or ceritinib for 48 and 72 h. Results shown are representative of three independent experiments

the prolonged treatments (Fig. 4e). Meanwhile, similar inhibitory effects showed on ALK^{ATI}-expressing U2197 and SK-LMS-1 cells (Supplementary Fig. 2).

Moreover, to evaluate the therapeutic effect of ALK inhibitor on ALK^{ATI}-induced tumorigenesis in vivo, we transplanted HT1080 cells overexpressing ALK^{ATI} or vector into BALB/c nude mice and then treated the mice with crizotinib. Xenografts of HT1080 cells stably expressing ALK^{ATI} displayed faster growth rates and heavier weights than those of HT1080 xenografts expressing empty vector (Fig. 5a, b). Crizotinib treatment induced the regression of ALK^{ATI}-driven HT1080 xenografts. Furthermore, the mRNA expression levels of *c-Myc*, *ABCG2*, *BMI1*, *OCT4*, *CD44*, and *SOX2* in the ALK^{ATI}-driven HT1080 xenografts were higher than those in vector-driven HT1080 xenografts. The expression of these stem cell markers was significantly decreased after crizotinib treatment (Fig. 5c). In addition, we detected the expression of c-Myc in explanted xenografts by IHC and confirmed that c-Myc labeling in the ALK^{ATI}-driven HT1080 cells xenografts was stronger than the labeling in the vector-driven HT1080 xenografts. In addition, this labeling was significantly reduced after crizotinib treatment (Fig. 5d).

To summarize, these findings suggest that ALK inhibitors suppress ALK^{ATI}-driven tumorigenesis as well as the expression of ALK^{ATI}-induced stem cell markers both in vitro and in vivo.

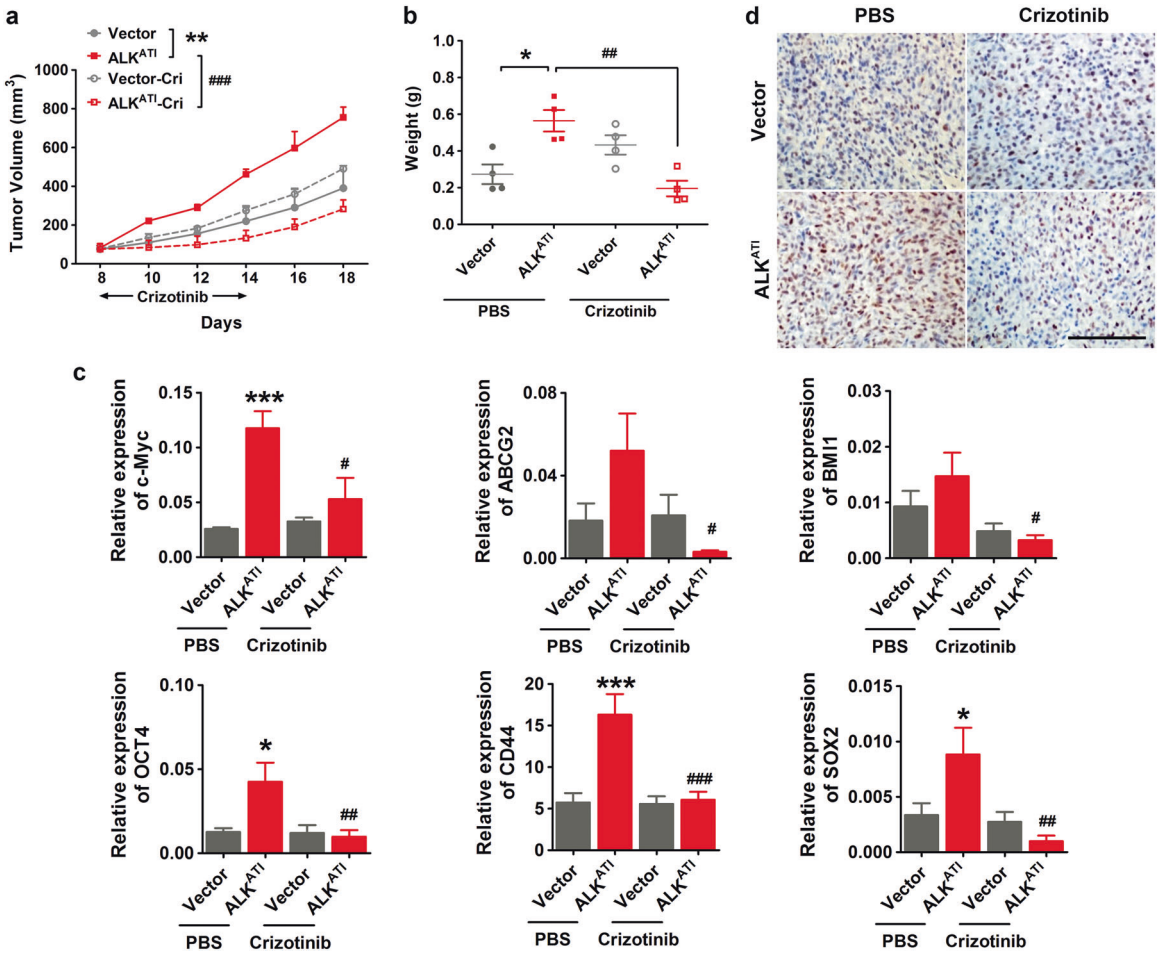

Fig. 5 Inhibitory effect of crizotinib on HT1080 xenografts expressing *ALK*^{ATI}. The tumor growth curve (**a**) and weight (**b**) of nude mice implanted with HT1080 cells stably expressing *ALK*^{ATI} or empty vector were orally gavaged once a day with crizotinib (100 mg/kg per day) or vehicle (1 × PBS, 200 µL per day) for 7 days; $n = 4$ mice per group. **c** Real-time PCR detection of stem cell markers in HT1080 xenografts expressing *ALK*^{ATI} or empty vector after crizotinib treatment. All mice were killed four days after drug withdrawal and xenografts were explanted and preserved for RNA extraction, reverse transcription, and real-time PCR detection; $n = 4$ mice per group. Data are shown as mean ± SD. $^{*}P < 0.05$, $^{**}P < 0.01$, $^{***}P < 0.001$ vs. Vector group; hash refers to differences between PBS and crizotinib treatment, $^{\#}P < 0.05$, $^{\#\#}P < 0.01$, $^{\#\#\#}P < 0.001$ vs. *ALK*^{ATI} group treated with PBS by one-way ANOVA analysis followed by Bonferroni post hoc test (**a**) or two-tailed Student's *t*-test (**b**, **c**). Results shown are representative of three independent*t* experiments. **d** Immunohistochemical staining for c-Myc in HT1080 xenografts expressing *ALK*^{ATI} or empty vector after crizotinib treatment. Xenografts were explanted and fixed overnight in 4% paraformaldehyde, washed, embedded in paraffin, and sectioned for c-Myc immunohistochemical staining. Magnification: ×200; bar: 100 µm

ALK^{ATI} interacted with c-Myc and promoted the binding of c-Myc to the ABCG2 promoter

Considering the data above, we speculated that stronger stem cell-like properties induced by *ALK*^{ATI} may due to the nuclear expression of ALK^{ATI}. It is possible that ALK^{ATI} is transferred into the nucleus and interacts with transcription factors such as c-Myc, ABCG2, or BMI1. Each of these transcription factors are also stem cell biomarkers and are highly expressed in *ALK*^{ATI}-expressing HT1080 cells. As c-Myc has been reported to be an important gene related to chemosensitivity and radioresistance in sarcomas [26, 27], we then examined the possibility of an interaction between ALK^{ATI} and c-Myc. First, we detected the co-localization of ALK^{ATI} and c-Myc in *ALK*^{ATI}-expressing HT1080 cells and found that ALK^{ATI} was co-expressed with c-Myc in the nuclei of HT1080 cells (Fig. 6a). The co-localization of ALK^{ATI} and c-Myc was then confirmed by immunofluorescence in 293 T cells expressing *ALK*^{ATI}-*Flag* and *c-Myc-HA* plasmids (Fig. 6b). To investigate whether ALK^{ATI} interacts with c-Myc, we performed co-immunoprecipitation in 293 T cells expressing *ALK*^{ATI}-*Flag* and *c-Myc-HA* plasmids (or *ALK*^{WT}-*Flag* and *c-Myc-HA* plasmids as a control). There was a significant interaction between ALK^{ATI} and c-Myc in *ALK*^{ATI}-expressing

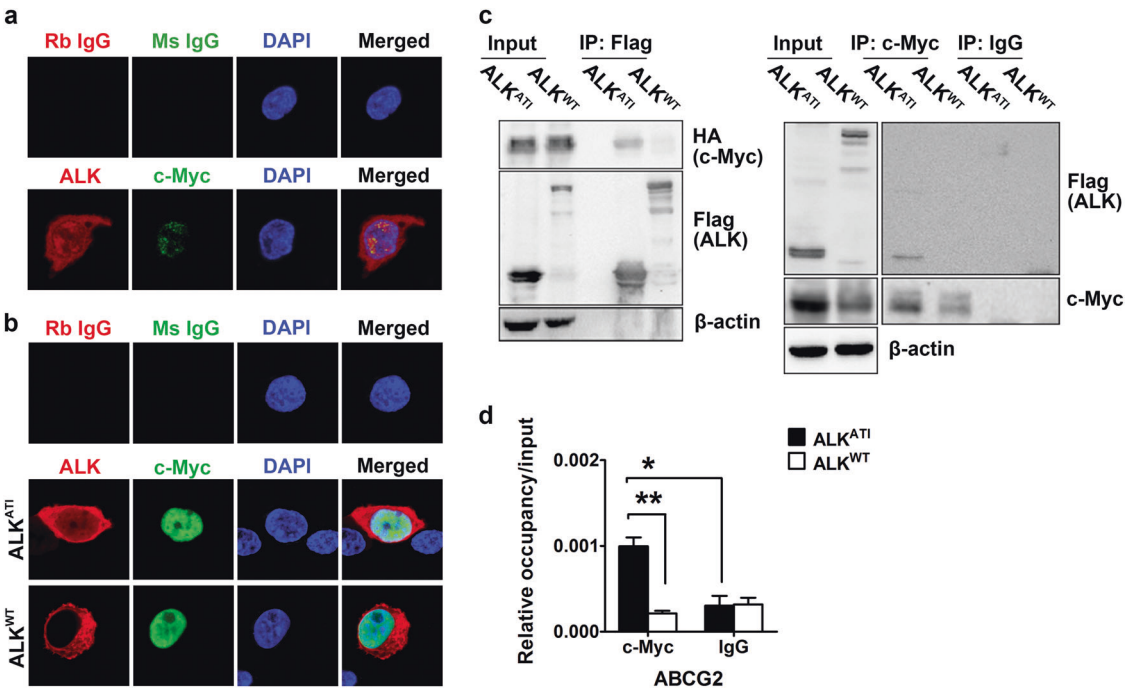

Fig. 6 The interaction between ALK^{ATI} and c-Myc promoted the binding of c-Myc to *ABCG2* promoter. **a** Immunofluorescent staining of ALK^{ATI} (red) and c-Myc (green) in HT1080 cells stably expressing *ALK*^{ATI}. Nuclei were stained with DAPI (blue). Rabbit and mouse IgG served as negative controls. Original magnification: ×600. **b** Immunofluorescent staining of ALK^{ATI} (red) and c-Myc (green) in 293 T cells transiently transfected with *ALK*^{ATI} and *c-Myc* or *ALK*^{WT} and *c-Myc* plasmids. Nuclei were stained with DAPI (blue). Rabbit and mouse IgG served as negative controls. Original magnification: ×600. **c** Detection of the interaction of ALK^{ATI} with c-Myc via immunoprecipitation with an anti-Flag antibody (left panel) or anti-c-Myc antibody (right panel) in 293 T cells transiently transfected with *ALK*^{ATI} and *c-Myc* or *ALK*^{WT} and *c-Myc* plasmids. Immunoprecipitation with rabbit IgG served as a negative control. Representative western blotting images are shown for ALK, c-Myc, and β-actin protein expression. The input served as a positive control. **d** Binding of c-Myc to the *ABCG2* promoter was enhanced by *ALK*^{ATI}. ChIP assays were performed using an antibody against c-Myc in HT1080 cells stably expressing *ALK*^{ATI} or *ALK*^{WT} and real-time PCR was used to quantify the levels of amplified DNA. Rabbit IgG served as a negative control; Data are shown as mean ± SD. $^{*}P < 0.05$ and $^{**}P < 0.01$ using two-tailed Student's *t*-test. Results shown are representative of three independent experiments

293 T cells (Fig. 6c). The interaction between ALK^{ATI} and c-Myc was then confirmed via reverse co-immunoprecipitation assays (Fig. 6c, right panel). We next investigated whether the interaction between ALK^{ATI} and c-Myc affects the stem cell-related transcriptional regulation of c-Myc. We performed Chromatin immunoprecipitation (ChIP) assays to examine the interaction of c-Myc with the promoters of stem cell markers in HT1080 cells overexpressing either *ALK*^{ATI} or wild-type *ALK*. As a result, we found that ALK^{ATI} induced significantly greater binding of c-Myc to the *ABCG2* promoter (Fig. 6d). Hence, these results suggest that ALK^{ATI} is transferred into the nucleus and interacts with c-Myc, promoting the binding of c-Myc to the *ABCG2* promoter and resulting in stronger stem cell-like properties.

Discussion

ALK kinase activation through overexpression or translocation correlates with advanced clinical stage and poor prognosis in several tumor types [28, 29]. Sporadic cases show that STS patients carrying *ALK* fusion genes such as *RANBP2-ALK* or *TPM3-ALK* benefit from treatment with ALK inhibitors [16, 18]. We also found that *ALK*^{ATI} occurs frequently in multiple types of sarcomas and its expression was associated with advanced tumor grade and a significantly lower probability of PFS, suggesting that the new *ALK* transcript may be a novel prognostic predictor for STS patients and thus worth further investigation.

ALK^{ATI} was first identified by RNA sequencing [21]. Here, we used a real-time PCR assay with specific probe and primers to detect *ALK*^{ATI} expression and found that *ALK*^{ATI} mRNA expressed higher (31.58%) in multiple types of STS as compared with melanomas (~11%) [21], which may partly due to the sensitivity and specificity of the detection method. Moreover, we confirmed that *ALK*^{ATI} expressed both in the nucleus and cytoplasm in vitro, which was consistent with a previous report [21]. Although the occurrence rate of *ALK*^{ATI} in STS should be confirmed in a larger sarcoma cohort using a more sensitive and specific

method, our findings indicate that *ALK*^{ATI} is present in and may play an important role in the development of STS.

ALK kinase activation usually stimulates multiple oncogenic signaling pathways, resulting in the growth and survival of tumor cells [9]. However, compared with wild-type *ALK* and *NPM- ALK*, *ALK*^{ATI} not only contributes to tumor cell growth and proliferation but also promotes CSC-like properties in sarcoma cells. CSCs are considered to be responsible for recurrence, metastasis, and resistance to chemotherapy and radiotherapy in some cancers [30–33]. CSCs are proposed to originate from a transformed stem cell or committed cell with genetic alterations that provide unlimited proliferation [23, 24, 34]. In fact, some genetic variations that might result in malignant cell proliferation have been identified in various types of tumors, including STS [35, 36]. The links between *ALK* aberrations and CSC biology have not yet been reported. Here, we provide the first evidence that *ALK*^{ATI} promotes CSC-like properties in sarcoma cell lines by enhancing sphere formation and upregulating the expression of stem cell markers (including *c-Myc*, *ABCG2*, *BMI1*, and *CD44*), which also induced chemoresistance and radioresistance. Furthermore, cells dissociated from the *ALK*^{ATI}-expressing sarcoma sphere primary cells were shown to be capable of repeatedly forming spheres. The capacity for subcultured sphere formation has been demonstrated in a population of CD133^{+} HT1080 cells [37]. Taken together, our results suggest that *ALK*^{ATI} might play a significant role in carcinogenesis by enhancing CSC-like properties.

Crizotinib can inhibit *ALK*^{ATI}-induced proliferation and tumorigenesis [21]. Here, we demonstrated that ALK inhibitors not only suppressed the proliferation and tumorigenesis of *ALK*^{ATI}-expressing sarcoma cells but also declined the phosphorylation of ALK^{ATI} and the downstream effectors. Furthermore, we exhibited that ALK inhibitors down-regulated the expression of stem cell markers such as *c-Myc*, *ABCG2*, *BMI1*, and *CD44* both in vitro and in vivo. The AKT/mTOR signaling pathway could modulate the expression of stem cell markers [38, 39] and the suppression of stem cell markers expression by ALK inhibitors may decline its downstream pathway activation. In addition, it has been reported that the identified *ALK* translocations and the mutation can induce the overexpression of ALK protein and the activation of downstream PI3K/AKT, MAPK, and STAT3/5 signaling pathways, resulting in a malignant phenotype and the proliferation and survival of tumor cells [9]. Our studies demonstrated the different downstream pathway that *ALK*^{ATI} activated.

The transcription factor c-Myc is a key regulator involved in sustaining CSC properties [40–42]. There is evidence that c-Myc maintains transformed phenotypes and induces radioresistance by suppressing radiation-induced apoptosis and DNA damage, promoting radiation-induced DNA repair in embryonal rhabdomyosarcoma cell lines [27]. c-Myc can also induce chemoresistance through transcriptional regulation of ABC transporter family genes, especially *ABCG2* [43, 44]. In this study, we found that ALK^{ATI} was co-expressed with c-Myc in HT1080 cells; ALK^{ATI} interacted with c-Myc and promoted the binding of c-Myc to the *ABCG2* promoter. Combined with the findings that *ALK*^{ATI}-expressing HT1080 cells possess stronger radioresistant and chemoresistant abilities than controls and that overexpression of *ALK*^{ATI} resulted in the upregulation of c-Myc and ABCG2, it is easy to deduce that the CSC-like properties induced by *ALK*^{ATI} might result from the interaction of ALK^{ATI} and c-Myc and the following downstream transcriptional events. Other mechanisms of induction of CSC-like properties by *ALK*^{ATI} require further investigation.

In summary, we demonstrated that the new *ALK* transcript *ALK*^{ATI} occurs frequently in STS and *ALK*^{ATI} expression is associated with a poor prognosis. Furthermore, we provided the first evidence that *ALK*^{ATI} promotes CSC-like properties in sarcoma cells, at least in part via interactions with c-Myc that promotes the binding of c-Myc to the *ABCG2* promoter. These findings implicate *ALK*^{ATI} as a potential prognostic biomarker and therapeutic target for STS.

Materials and methods

Patients and specimens

All clinical samples were collected from Sun Yat-sen University Cancer Center, Guangzhou, China. A total of 38 sarcoma biopsy specimens were collected between August 2012 and January 2016 for real-time PCR assays. Clinical follow-up was available for these cases. A total of 142 paraffin-embedded sarcoma specimens were collected for IHC analyses between 2000 and January 2010.

Antibodies

Primary antibodies against Flag (#F1804, Sigma-Aldrich, USA), HA (#sc-805, Santa Cruz Biotechnology, USA), Myc (#OP10, Millipore, USA), β-actin (#66009-1-1 g, Proteintech Group Inc., USA), phospho-ALK-Tyr1604 (#3341, Cell Signaling, USA), phospho-AKT1-Ser473 (#4060, Cell Signaling, USA), phospho-ERK1/2 -Thr202/Tyr204 (#4376, Cell Signaling, USA); phospho-mTOR-Ser2448 (#5536 s, Cell Signaling, USA), ALK (#3633, Cell Signaling, USA), AKT (#KC-5A01, Kangcheng Biotech., China), ERK1/2 (#KC-5E01, Kangcheng Biotech., China), mTOR (#2983 s, Cell Signaling, USA), ABCG2 (#ab3380, Abcam, UK), OCT4 (#2750 s, Cell Signaling, USA), c-Myc (#9402 s, Cell Signaling, USA; #ab32072, Abcam, UK), BMI1 (#2933, Cell Signaling, USA), and normal mouse/

rabbit IgG (R&D Systems, USA) were obtained accordingly. Secondary antibodies include HRP-conjugated goat-anti-mouse/rabbit antibodies (Fisher Scientific, USA) and fluorescein-conjugated goat-anti-mouse/rabbit antibodies (Molecular Probes, USA).

Cell culture

The human fibrosarcoma cell line (HT1080), human undifferentiated pleomorphic sarcoma cell line (U2197), and human leiomyosarcoma cell line (SK-LMS-1), as well as 293 T cells were cultured using DMEM (Gibco, USA) supplemented with 10% fetal bovine serum (FBS) (Gibco, USA) in a humidified incubator containing 5% CO2 at 37 °C. Cell line authentication was performed (Microread Co., Beijing, China) and tested for mycoplasma contamination.

Plasmids construction

ALK^{ATI} was amplified from STS tissue cDNA as descried previously [21], and then subcloned into a pBabe-puro vector (Invitrogen, USA) by ClonExpress II One Step Cloning Kit (#C112-02, Vazyme, China). The full-length *ALK* (*ALK*^{WT}) and *NPM-ALK* plasmids were kindly provided by Dr Deng Xianming. Plasmids were subcloned into pBabe-puro vectors and confirmed by direct sequencing. For co-immunoprecipitation, *ALK*^{ATI}*-Flag* and *ALK*^{WT}*-Flag* were subcloned into a pcDNA3.1 (+) vector (Invitrogen, USA). *C-Myc-HA* was amplified from HT1080 cDNA and then also subcloned into a pcDNA3.1(+) vector (Invitrogen, USA).

Establishment of stable cell lines

Retrovirus was produced in 293 T cells according to the manufacturer's instructions. The virus-containing supernatant was harvested 48 h after transfection and used for transduction in the presence of polybrene (8 mg/ml, Sigma-Aldrich, USA). HT1080, U2197, and SK-LMS-1 cells expressing *ALK*^{ATI}, *ALK*^{WT}, *NPM-ALK*, or empty vector were selected with puromycin (Sigma-Aldrich, USA) for 7–10 days after infection with retrovirus for 48 h. After selection, the generation of *ALK*^{ATI}, *ALK*^{WT}, *NPM-ALK*, and empty vector-expressing stable cell lines was verified, and the resulting cells were cultured in fresh medium.

Quantitative real-time PCR analysis

Total RNA was extracted from sarcoma biopsy specimens and various cell lines using TRIZOL reagent (Sigma-Aldrich, USA). First-strand cDNA was synthesized from 1 μg of total RNA using Superscript III Reverse Transcriptase (Invitrogen, USA). The presence of *ALK*^{ATI} in sarcoma biopsies was detected using a Taqman Gene Expression Assay (Applied Biosystems, USA) on an LC480 Real-Time PCR system (Roche, Switzerland). The amplification of *ALK*^{ATI} was further confirmed by direct sequencing. The following sequence-specific probe and two primers constructed for *ALK* intron 19 and exons 20–29 were used:

ALK^{ATI}-probe: 5′-FAM-CATGTTGCAGCTGACCA-3′-MGB

ALK^{ATI}-forward: 5′-GAGATCCAGGGAGGCTTCCT-3′

ALK^{ATI}-reverse: 5′-GCCCAGACCCCGAATGAG-3′

ALK^{ATI} quantifications were performed simultaneously with PCR amplified standards using tenfold serial dilutions of the *ALK*^{ATI} plasmid and no-template controls.

Regarding the detection of stem cell markers, real-time PCR was performed with iQTM SYBR Green Supermix (Bio-Rad, USA) according to the manufacturer's instructions. The primers of stem cell markers are listed in Supplementary Table 2. Expression data were normalized to the geometric mean of the housekeeping gene *β-actin* and calculated as $2^{-}\Delta^{\Delta_{CT}}$.

Sphere formation assay

Three hundred stably transduced sarcoma cells were cultured in FBS-free DMEM/F12 medium (Invitrogen, USA) supplemented with B-27 (1 mL/50 mL of medium, Invitrogen, USA), human recombinant EGF (20 ng/mL, Invitrogen, USA), and bFGF (20 ng/mL, Invitrogen, USA) on ultra-low attachment 24-well plates for 14 days; the media were changed every 3 days. The capacity for subcultured sphere formation was also investigated by repeated dissociation using 0.02% EDTA followed by subculture in the same conditions on ultra-low attachment 24-well plates. Sphere formation cells were then collected and used for real-time PCR assays.

IHC assay

IHC was performed on archival formalin-fixed paraffin-embedded tumor specimens with the anti-ALK or anti-c-Myc (#ab32072, Abcam, UK) antibodies using a Dako REAL™ EnVision™ Detection System according to the manufacturer's instructions (Agilent, Denmark). Images were observed under ×200 and ×400 magnifications using a motorized microscope (Olympus Inc., Japan). Semi-quantitative analysis was used to score the staining intensity as follows: 0, negative staining; 1+, weak staining; 2+, moderate staining; and 3+, strong staining.

Immunofluorescence staining

Stable HT1080 cell lines were grown on coverslips (Costar, Cambridge, MA) in 24-well plates and cultured for 24 h to allow the cells to reach confluence. The cells were then fixed with 4% paraformaldehyde (PFA) in 1 × PBS (pH 7.4) at room temperature for 15 min and blocked for 1 h with 3% BSA and 0.1% Triton X-100 in 1 × PBS at room temperature. After blocking, cells were incubated with a primary ALK mAb (Cell Signaling Technology, 1:200 dilution) overnight at 4 °C. To assess the co-localization of ALK with c-Myc, the cells were incubated with a primary rabbit anti-ALK mAb and a primary mouse anti-Myc mAb (#OP10, Millipore, USA, 1:100 dilution) overnight at 4 °C. Subsequently, cells were incubated with the indicated fluorescein-conjugated secondary antibodies (Invitrogen, 1:1000 dilution) at 37 °C for 1 h. Then, slides were mounted in DAPI for nuclear staining, and fluorescence images were obtained using a confocal laser-scanning microscope in the sequential scan mode (FV-100, Olympus Inc., Japan).

Co-immunoprecipitation

ALK^{ATI}*-Flag*, *ALK*^{WT}*-Flag*, and *c-Myc-HA* plasmids were transiently transfected into 293 T cells using Lipofectamine 3000 transfection reagent (Invitrogen, USA). After 24 h, cells were collected and resuspended in IP buffer (Beyotime Institute Biotech, China) and lysed by ultrasonication on ice. After incubation and centrifugation, 100 µL supernatant was used as input and 500 µL was used for immunoprecipitation using the following antibodies: 30 µL of ANTI-FLAG® M2 Affinity Agarose Gel (Sigma-Aldrich, USA), anti-c-Myc antibody (#9402 s, Cell Signaling, USA), and normal rabbit IgG control. We used 30 µL of Pierce™ protein A/G Agarose (Thermo Scientific, USA) for immunoprecipitation. The immunoprecipitated material was eluted in 4 × SDS loading buffer for immunoblotting.

Western blotting

ALK^{ATI}-expressing or pBabe empty vector-carrying stable sarcoma cells were seeded in 12-well plates and treated with various concentrations of crizotinib (Sigma-Aldrich, USA) or ceritinib (Selleck, USA) for 3 h (to determine the phosphorylation levels of both ALK and its downstream effectors) and for 24 h, 48 h or 72 h (to detect the expression of stem cell markers). Total protein was harvested, separated by SDS-PAGE, and electrophoretically transferred to PVDF membranes (Pall, Port Washington, NY, USA). The membranes were blocked in 5% nonfat dry milk as necessary, followed by incubation with the corresponding primary antibodies at 4 °C overnight. After washing with TBST (1 × TBS + 0.1% Tween-20), the membranes were incubated with HRP-conjugated secondary antibodies for 45 min at room temperature. After three washes, immunoblots were visualized via enhanced chemiluminescence (Amersham, UK). β-actin was used as a protein loading control.

MTT assay

Cells were seeded in 96-well plates at 1000 cells/well and incubated overnight. Each sample was examined in at least five replicates. Cells were incubated with 0.2% MTT (5 mg/mL) for 4 h at 37 °C. Then, 100 µL of DMSO was added to each well to dissolve the crystals and cells were counted every day by measuring absorbance at 490 nm. For the half-maximal inhibitory concentration (IC_{50}) value determination, cells were treated on day 2 with various concentrations of crizotinib or ceritinib for 48 h. The IC_{50} was calculated based on a survival curve.

Colony formation assay

To investigate the growth, cells were seeded in six-well plates at 200 cells/well and incubated in the media which was replaced every 2–3 days. And for the drug effects, cells were seeded in six-well plates at 1000 cells/well and incubated overnight, then treated with an IC_{25}–IC_{50} concentration of crizotinib or ceritinib. Two days after chemical treatment, the media were replaced with fresh media. Seven to ten days later, the cells were fixed with methanol for 10 min and stained with 0.5% crystal violet for 15 min. Triplicate wells were set up for each condition.

In vivo tumorigenicity and drug studies

Specific pathogen-free (SPF), 4–6-week-old, female BALB/c nude mice ($n = 16$) were purchased from Beijing Vital River Laboratory Animal Technology Co., Ltd. (Beijing, China) and maintained in an SPF facility. Mice were given a subcutaneous injection of 200 µL of a viable cell suspension mixture (1×10^6 cells) containing 75% cell suspension and 25% Matrigel (Corning, USA). When the tumors reached an average size of 100–150 mm^3, mice were randomized into vehicle or treatment groups (four mice per group). Mice were orally gavaged once a day with crizotinib (100 mg/kg per day) or vehicle (PBS, 200 µL per day) for 7 days (days 8–14). Tumor dimensions were measured with calipers every 2 days, without blinding, and volumes were calculated using the following formula: tumor volume $= (D \times d^2)/2$, where D and d refer to the long and short tumor diameter, respectively. All mice were killed 4 days after drug withdrawal and tumors were explanted and weighed. Tumors were then either preserved for RNA extraction or fixed for IHC. Mouse experiments were performed once. All animal studies were approved by the Institutional Research Medical Ethics

Committee of Sun Yat-Sen University Cancer Center. Ethical approval was given by the Institutional Research Medical Ethics Committee of Sun Yat-Sen University Cancer Center.

ChIP assay

ChIP assays were performed using a Pierce Magnetic ChIP kit (Thermo Scientific, USA) according to the manufacturer's instructions. Briefly, cells were cross-linked with 1% formaldehyde and then harvested for cell lysis and MNase digestion. Equal amounts of an anti-c-Myc antibody (#9402 s, Cell Signaling, USA) and normal rabbit IgG were added, and the mixture was rotated overnight at 4 °C. Subsequently, Protein A/G magnetic beads were added, and the mixture was rotated for 2 h at 4 °C. After washing the beads, the precipitated immunocomplexes were eluted, and DNA was recovered using the DNA Clean-Up Column provided with the kit. Purified DNA was employed for real-time PCR. The primers used for qPCR in the ChIP assay were as follows:

ABCG2-Promoter-forward:
5′-AGGCGGGAGTGTTTGGCTTGT-3′
ABCG2-Promoter-reverse:
5′-CCTGCGACCCGGCTGAAA-3′
ABCG2-NC-Promoter-forward:
5′-TAAATGCCAGTATCCCACTCAG-3′
ABCG2-NC-Promoter-reverse:
5′-CATCATCATAGGAAAGCGAAGC-3′

The site of c-Myc binding to the *ABCG2* promoter was predicted using the QIAGEN website (Available online: http://saweb2.sabiosciences.com/chipqpcrsearch.php?app=gene). Primers designed ~8000 bp upstream of the predicted *ABCG2* promoter site were used for the NC.

Statistical analysis

All of the statistical analyses were performed using SPSS standard version 16.0 (SPSS Inc., Chicago, USA) and GraphPad Prism version 5.0 (GraphPad Software, San Diego, CA, USA). One-way analysis of variance (ANOVA) was used to compare differences between groups. A two-tailed Student's *t*-test was used when only two testing groups were analyzed. The associations between ALK^{ATI} mRNA expression and specific clinical characteristics were analyzed by Pearson's chi-squared test or Fisher's exact test. Disease-specific survival analysis was performed by Kaplan–Meier and Log-rank test. All data have been tested for normal distribution and equal variance. *P*-values <0.05 were considered statistically significant.

Acknowledgements This work was supported by the National Key Research and Development Program (2017YFA0505600) and the National Natural Science Foundation of China Programs (Grant Nos 81772863 and 81572403). We thank Dr Deng Xianming (Principal Investigator for Chemical Biology and Medicinal Chemistry School of Life Sciences, Xiamen University, China) for generously providing the plasmids.

Compliance with ethical standards

Conflict of interest The authors declare that they have no conflict of interest.

Publisher's note: Springer Nature remains neutral with regard to jurisdictional claims in published maps and institutional affiliations.

References

1. Toro JR, Travis LB, Wu HJ, Zhu K, Fletcher CD, Devesa SS. Incidence patterns of soft tissue sarcomas, regardless of primary site, in the surveillance, epidemiology and end results program, 1978–2001: an analysis of 26,758 cases. Int J Cancer. 2006;119:2922–30.
2. Pisters PW, Leung DH, Woodruff J, Shi W, Brennan MF. Analysis of prognostic factors in 1041 patients with localized soft tissue sarcomas of the extremities. J Clin Oncol. 1996;14:1679–89.
3. Lewis JJ, Leung D, Heslin M, Woodruff JM, Brennan MF. Association of local recurrence with subsequent survival in extremity soft tissue sarcoma. J Clin Oncol. 1997;15:646–52.
4. FDA Approval for Pazopanib Hydrochloride. U.S. National Institutes of Health, 2013. https://www.cancer.gov/about-cancer/treatment/drugs/fda-pazopanibhydrochloride. Accessed 28 Sep 2017.
5. FDA approves new therapy for certain types of advanced soft tissue sarcoma. U.S. Food and Drug Administration, 2015. https://www.fda.gov/NewsEvents/Newsroom/PressAnnouncements/ucm468832.htm. Accessed 18 Aug 2017.
6. FDA approves first drug to show survival benefit in liposarcoma. U.S. Food and Drug Administration, 2016. https://www.fda.gov/NewsEvents/Newsroom/PressAnnouncements/ucm483714.htm. Accessed 18 Aug 2017.
7. FDA grants accelerated approval to new treatment for advanced soft tissue sarcoma. U.S. Food and Drug Administration, 2016. www.fda.gov/NewsEvents/Newsroom/PressAnnouncements/ucm525878.htm. Accessed 18 Aug 2017.
8. Sheng JY, Movva S. Systemic therapy for advanced soft tissue sarcoma. Surg Clin North Am. 2016;96:1141–56.
9. Grande E, Bolos MV, Arriola E. Targeting oncogenic ALK: a promising strategy for cancer treatment. Mol Cancer Ther. 2011;10:569–79.
10. Armstrong F, Lamant L, Hieblot C, Delsol G, Touriol C. TPM3-ALK expression induces changes in cytoskeleton organisation and confers higher metastatic capacities than other ALK fusion proteins. Eur J Cancer. 2007;43:640–6.
11. Shaw AT, Yeap BY, Mino-Kenudson M, Digumarthy SR, Costa DB, Heist RS, et al. Clinical features and outcome of patients with non-small-cell lung cancer who harbor EML4-ALK. J Clin Oncol. 2009;27:4247–53.
12. Van Roosbroeck K, Cools J, Dierickx D, Thomas J, Vandenberghe P, Stul M, et al. ALK-positive large B-cell lymphomas with cryptic SEC31A-ALK and NPM1-ALK fusions. Haematologica. 2010;95:509–13.
13. Janoueix-Lerosey I, Lequin D, Brugieres L, Ribeiro A, de Pontual L, Combaret V, et al. Somatic and germline activating mutations of the ALK kinase receptor in neuroblastoma. Nature. 2008;455:967–70.

14. Bonvini P, Zin A, Alaggio R, Pawel B, Bisogno G, Rosolen A. High ALK mRNA expression has a negative prognostic significance in rhabdomyosarcoma. Br J Cancer. 2013;109:3084–91.
15. Ishibashi Y, Miyoshi H, Hiraoka K, Arakawa F, Haraguchi T, Nakashima S, et al. Anaplastic lymphoma kinase protein expression, genetic abnormalities, and phosphorylation in soft tissue tumors: Phosphorylation is associated with recurrent metastasis. Oncol Rep. 2015;33:1667–74.
16. Kimbara S, Takeda K, Fukushima H, Inoue T, Okada H, Shibata Y, et al. A case report of epithelioid inflammatory myofibroblastic sarcoma with RANBP2-ALK fusion gene treated with the ALK inhibitor, crizotinib. Jpn J Clin Oncol. 2014;44:868–71.
17. Jiang Q, Tong HX, Hou YY, Zhang Y, Li JL, Zhou YH, et al. Identification of EML4-ALK as an alternative fusion gene in epithelioid inflammatory myofibroblastic sarcoma. Orphanet J Rare Dis. 2017;12:97.
18. Mansfield AS, Murphy SJ, Harris FR, Robinson SI, Marks RS, Johnson SH, et al. Chromoplectic TPM3-ALK rearrangement in a patient with inflammatory myofibroblastic tumor who responded to ceritinib after progression on crizotinib. Ann Oncol. 2016;27:2111–7.
19. Subbiah V, McMahon C, Patel S, Zinner R, Silva EG, Elvin JA, et al. STUMP un"stumped": anti-tumor response to anaplastic lymphoma kinase (ALK) inhibitor based targeted therapy in uterine inflammatory myofibroblastic tumor with myxoid features harboring DCTN1-ALK fusion. J Hematol Oncol. 2015;8:66.
20. Lee JC, Li CF, Huang HY, Zhu MJ, Marino-Enriquez A, Lee CT, et al. ALK oncoproteins in atypical inflammatory myofibroblastic tumours: novel RRBP1-ALK fusions in epithelioid inflammatory myofibroblastic sarcoma. J Pathol. 2017;241:316–23.
21. Wiesner T, Lee W, Obenauf AC, Ran L, Murali R, Zhang QF, et al. Alternative transcription initiation leads to expression of a novel ALK isoform in cancer. Nature. 2015;526:453–7.
22. Busam KJ, Vilain RE, Lum T, Busam JA, Hollmann TJ, Saw RP, et al. Primary and metastatic cutaneous melanomas express ALK through alternative transcriptional initiation. Am J Surg Pathol. 2016;40:786–95.
23. Clevers H. The cancer stem cell: premises, promises and challenges. Nat Med. 2011;17:313–9.
24. Beck B, Blanpain C. Unravelling cancer stem cell potential. Nat Rev Cancer. 2013;13:727–38.
25. Deshmukh A, Deshpande K, Arfuso F, Newsholme P, Dharmarajan A. Cancer stem cell metabolism: a potential target for cancer therapy. Mol Cancer. 2016;15:69.
26. Xie X, Ye Z, Yang D, Tao H. Effects of combined c-myc and Bmi-1 siRNAs on the growth and chemosensitivity of MG-63 osteosarcoma cells. Mol Med Rep. 2013;8:168–72.
27. Gravina GL, Festuccia C, Popov VM, Di Rocco A, Colapietro A, Sanita P, et al. c-Myc sustains transformed phenotype and promotes radioresistance of embryonal rhabdomyosarcoma cell lines. Radiat Res. 2016;185:411–22.
28. Schulte JH, Bachmann HS, Brockmeyer B, Depreter K, Oberthur A, Ackermann S, et al. High ALK receptor tyrosine kinase expression supersedes ALK mutation as a determining factor of an unfavorable phenotype in primary neuroblastoma. Clin Cancer Res. 2011;17:5082–92.
29. Zhou JX, Yang H, Deng Q, Gu X, He P, Lin Y, et al. Oncogenic driver mutations in patients with non-small-cell lung cancer at various clinical stages. Ann Oncol. 2013;24:1319–25.
30. Todaro M, Francipane MG, Medema JP, Stassi G. Colon cancer stem cells: promise of targeted therapy. Gastroenterology. 2010;138:2151–62.
31. Dandawate PR, Subramaniam D, Jensen RA, Anant S. Targeting cancer stem cells and signaling pathways by phytochemicals: novel approach for breast cancer therapy. Semin Cancer Biol. 2016;40-41:192–208.
32. Brown HK, Tellez-Gabriel M, Heymann D. Cancer stem cells in osteosarcoma. Cancer Lett. 2017;386:189–95.
33. Fujiwara T, Ozaki T. Overcoming therapeutic resistance of bone sarcomas: overview of the molecular mechanisms and therapeutic targets for bone sarcoma stem cells. Stem Cells Int. 2016;2016:2603092.
34. Kuo CY, Ann DK. When fats commit crimes: fatty acid metabolism, cancer stemness and therapeutic resistance. Cancer Commun (Lond). 2018;38:47.
35. Riggi N, Cironi L, Provero P, Suva ML, Kaloulis K, Garcia-Echeverria C, et al. Development of Ewing's sarcoma from primary bone marrow-derived mesenchymal progenitor cells. Cancer Res. 2005;65:11459–68.
36. Haldar M, Hancock JD, Coffin CM, Lessnick SL, Capecchi MR. A conditional mouse model of synovial sarcoma: insights into a myogenic origin. Cancer Cell. 2007;11:375–88.
37. Feng BH, Liu AG, Gu WG, Deng L, Cheng XG, Tong TJ, et al. CD133+ subpopulation of the HT1080 human fibrosarcoma cell line exhibits cancer stem-like characteristics. Oncol Rep. 2013;30:815–23.
38. Huang FF, Wu DS, Zhang L, Yu YH, Yuan XY, Li WJ, et al. Inactivation of PTEN increases ABCG2 expression and the side population through the PI3K/Akt pathway in adult acute leukemia. Cancer Lett. 2013;336:96–105.
39. Xia P, Xu XY. PI3K/Akt/mTOR signaling pathway in cancer stem cells: from basic research to clinical application. Am J Cancer Res. 2015;5:1602–9.
40. Kim J, Woo AJ, Chu J, Snow JW, Fujiwara Y, Kim CG, et al. A Myc network accounts for similarities between embryonic stem and cancer cell transcription programs. Cell. 2010;143:313–24.
41. Lin CY, Loven J, Rahl PB, Paranal RM, Burge CB, Bradner JE, et al. Transcriptional amplification in tumor cells with elevated c-Myc. Cell. 2012;151:56–67.
42. Wang Y, Cheng J, Xie D, Ding X, Hou H, Chen X, et al. NS1-binding protein radiosensitizes esophageal squamous cell carcinoma by transcriptionally suppressing c-Myc. Cancer Commun (Lond). 2018;38:33.
43. Porro A, Iraci N, Soverini S, Diolaiti D, Gherardi S, Terragna C, et al. c-MYC oncoprotein dictates transcriptional profiles of ATP-binding cassette transporter genes in chronic myelogenous leukemia CD34+ hematopoietic progenitor cells. Mol Cancer Res. 2011;9:1054–66.
44. Porro A, Haber M, Diolaiti D, Iraci N, Henderson M, Gherardi S, et al. Direct and coordinate regulation of ATP-binding cassette transporter genes by Myc factors generates specific transcription signatures that significantly affect the chemoresistance phenotype of cancer cells. J Biol Chem. 2010;285:19532–43.